

---

# On Calibration and Conformal Prediction of Deep Classifiers

---

Lahav Dabah<sup>1</sup> Tom Tirer<sup>1</sup>

## Abstract

In many classification applications, the prediction of a deep neural network (DNN) based classifier needs to be accompanied with some confidence indication. Two popular post-processing approaches for that aim are: 1) *calibration*: modifying the classifier’s softmax values such that their maximum (associated with the prediction) better estimates the correctness probability; and 2) *conformal prediction* (CP): devising a score (based on the softmax values) from which a set of predictions with theoretically guaranteed marginal coverage of the correct class is produced. While in practice both types of indications can be desired, so far the interplay between them has not been investigated. Toward filling this gap, in this paper we study the effect of temperature scaling, arguably the most common calibration technique, on prominent CP methods. We start with an extensive empirical study that among other insights shows that, surprisingly, calibration has a detrimental effect on popular adaptive CP methods: it frequently leads to larger prediction sets. Then, we turn to theoretically analyze this behavior. We reveal several mathematical properties of the procedure, according to which we provide a reasoning for the phenomenon. Our study suggests that it may be worthwhile to utilize adaptive CP methods, chosen for their enhanced conditional coverage, based on softmax values prior to (or after canceling) temperature scaling calibration.

(Miotto et al., 2018), autonomous vehicle decision-making (Grigorescu et al., 2020), and detection of security threats (Guo et al., 2018), where human lives are at risk.

In practice, DNN classification models typically generate a post-softmax vector, akin to a probability vector with nonnegative entries that add up to one. One might, intuitively, be interested in using the value associated with the prediction as the confidence (Cosmides & Tooby, 1996). However, this value often deviates substantially from the actual correctness probability. This discrepancy, known as *miscalibration*, is prevalent in modern DNN classifiers, which frequently demonstrate overconfidence: the maximal softmax value surpasses the true correctness probability (Guo et al., 2017). To address this issue, post-processing *calibration* methods are employed to adjust the values of the softmax vector. In particular, Guo et al. (2017) have demonstrated the usefulness of a simple Temperature Scaling (TS) procedure (a single parameter variant of Platt scaling (Platt et al., 1999)), which since then has gained massive popularity (Liang et al., 2018; Ji et al., 2019; Wang et al., 2021; Frenkel & Goldberger, 2021; Ding et al., 2021; Wei et al., 2022).

Another post-processing approach for uncertainty indication is Conformal Prediction (CP), which was originated in (Vovk et al., 1999; 2005) and has attracted much attention recently. CP algorithms are based on devising scores for all the classes per sample (based on the softmax values) that are used for producing a set of predictions instead of a single predicted class. In contrast to calibration techniques, CP algorithms have theoretical guarantees for coverage of the true class in the prediction set, assuming the data samples are exchangeable (e.g., the samples are i.i.d.).

Clearly, in critical applications, both types of confidence indications are desirable, as they provide complementary types of information that can lead to a comprehensive decision. Indeed, CP offers theoretically-backed set-based predictions, allowing for a nuanced understanding of uncertainty, but does not provide additional information for choosing a class from the set. Hence, whenever the prediction set size is larger than 1, a calibration method (such as TS) is essential for having a probability estimate for the correctness of the dominant class, which is aligned more accurately with its true likelihood. However, as far as we

## 1. Introduction

Modern classification systems are typically based on deep neural networks (DNNs) (Krizhevsky et al., 2012; He et al., 2016; Huang et al., 2017). In many applications, it is necessary to quantify and convey the level of uncertainty associated with each prediction of the DNN. This is particularly crucial in high-stakes scenarios, such as medical diagnoses

<sup>1</sup>Faculty of Engineering, Bar-Ilan University, Ramat Gan, Israel. Correspondence to: Lahav Dabah <lahavdabah@gmail.com>.

Preliminary work.

know, so far the interplay between calibration and CP has not been investigated.

Toward filling this gap, in this paper we study the effect of TS, arguably the most common calibration technique, on three prominent CP methods: Least Ambiguous set-valued classifier (LAC) (Lei & Wasserman, 2014; Sadinle et al., 2019), Adaptive Prediction Sets (APS) (Romano et al., 2020), and Regularized Adaptive Prediction Sets (RAPS) (Angelopoulos et al., 2021).

Our contributions can be summarized as follows:

- We conduct an extensive empirical study on DNN classifiers that shows that an initial TS calibration affects CP methods differently. Specifically, we show that its effect is negligible for LAC but, surprisingly, detrimental for the prediction sets sizes of the adaptive methods (APS and RAPS). Moreover, this behavior is more distinguishable in settings where the classifiers have limited accuracy.
- We theoretically study the tension between TS and the procedures of APS and RAPS. Specifically, we establish new results on effect of TS on the scores of APS and RAPS, according to which we provide a reasoning for the phenomenon.
- Our work challenges the conventional practice: calibrating DNNs before applying other post-processing algorithms. Specifically, our study demonstrates the advantage of utilizing adaptive CP methods based on softmax values before temperature scaling procedure.

## 2. Background and Related Work

Let us present the notations that are used in the paper, followed by some preliminaries on TS and CP.

We consider a  $C$ -classes classification task of the data  $(X, Y)$  distributed on  $\mathbb{R}^d \times [C]$ , where  $[C] := \{1, \dots, C\}$ . The classification is tackled by a DNN that for each input sample  $\mathbf{x} \in \mathbb{R}^d$  produces a logits vector  $\mathbf{z} = \mathbf{z}(\mathbf{x}) \in \mathbb{R}^C$  that is fed into a final softmax function  $\sigma : \mathbb{R}^C \rightarrow \mathbb{R}^C$ , defined as  $\sigma_i(\mathbf{z}) = \frac{\exp(z_i)}{\sum_{j=1}^C \exp(z_j)}$ . Typically, the post-softmax vector  $\hat{\pi}(\mathbf{x}) = \sigma(\mathbf{z}(\mathbf{x}))$  is being treated as an estimate of the class probabilities. Note that  $\hat{\pi}(\mathbf{x})$  is a valid probability vector: its entries are nonnegative and add up to 1. Equivalently, we can say  $\hat{\pi}(\mathbf{x}) \in \Delta^{C-1}$ , where  $\Delta^{C-1} := \{\pi : \pi_i \geq 0, \sum_{i=1}^C \pi_i = 1\}$  is the simplex in  $\mathbb{R}^C$ . The predicted class is given by  $\hat{y}(\mathbf{x}) = \operatorname{argmax}_i \hat{\pi}_i(\mathbf{x})$ .

Another notations that we use are  $\mathbb{I}(\cdot)$  to denote the indicator function,  $\mathbf{1}$  and  $\mathbf{0}$  to denote vectors of ones and zeros, respectively, and  $(x)_+ := \max\{x, 0\}$ .

### 2.1. Calibration and Temperature Scaling

The interpretation of  $\hat{\pi}(\mathbf{x})$  as an estimated class probabilities vector promotes treating  $\hat{\pi}_{\hat{y}(\mathbf{x})}(\mathbf{x})$  as the probability that the predicted class  $\hat{y}(\mathbf{x})$  is correct, which is also being referred to as the model’s confidence. However, it has been shown that DNNs are frequently overconfident —  $\hat{\pi}_{\hat{y}(x)}(x)$  is larger than the true correctness probability (Guo et al., 2017). Formally,  $\mathbb{P}(\hat{y}(X) = Y | \hat{\pi}_{\hat{y}(X)}(X) = p) < p$  with significant margin. Post-processing calibration techniques aim at reducing the aforementioned gap. They are based on optimizing certain transformations of the logits  $\mathbf{z}(\cdot)$ , yielding a probability vector  $\tilde{\pi}(\cdot)$  that minimizes a objective computed over a dedicated *calibration set* of labeled samples  $\{\mathbf{x}_i, y_i\}_{i=1}^n$  (Platt et al., 1999; Zadrozny & Elkan, 2002; Naeini et al., 2015).

One popular calibration objective is the Negative Log-Likelihood (NLL) (Hastie et al., 2005), given by  $\mathcal{L} = -\sum_{i=1}^n \ln(\tilde{\pi}_{y_i}(\mathbf{x}_i))$ , which measures the cross-entropy (dis-similarity) between the true conditional distribution of data (one-hot vector associated with  $y_i$ ) and  $\tilde{\pi}(\mathbf{x}_i)$ . Another popular objective is the Expected calibration error (ECE) (Naeini et al., 2015), which aims to approximate  $\mathbb{E}[|\mathbb{P}(\hat{y}(X) = Y | \tilde{\pi}_{\hat{y}(X)}(X) = p) - p|]$ . Specifically, the confidence range  $[0, 1]$  is divided into  $L$  equally sized bins  $\{B_l\}$ . Each sample  $(\mathbf{x}_i, y_i)$  is assigned to a bin  $B_l$  according to  $\tilde{\pi}_{y_i}(\mathbf{x}_i)$ . The objective is given by  $\text{ECE} = \sum_{l=1}^L \frac{|B_l|}{n} |\text{acc}(B_l) - \text{conf}(B_l)|$ , where  $\text{acc}(B_l) = \frac{1}{|B_l|} \sum_{i \in B_l} \mathbb{I}\{\hat{y}(\mathbf{x}_i) = y_i\}$  and  $\text{conf}(B_l) = \frac{1}{|B_l|} \sum_{i \in B_l} \tilde{\pi}_{y_i}(\mathbf{x}_i)$ . Other calibration metrics can be found, e.g., in (Nixon et al., 2019).

Temperature Scaling (TS) stands out as, arguably, the most common calibration approach, surpassing many others in achieving calibration with minimal computational complexity (Guo et al., 2017). It simply uses the transformation  $\mathbf{z} \mapsto \mathbf{z}/T$  before applying the softmax, where  $T > 0$  (the “temperature”) is a single scalar parameter that is set by minimizing the NLL or the ECE. Additionally, TS preserves the accuracy rate of the network (the ranking of the elements – and in particular, the index of the maximum – is unchanged), which may otherwise be compromised during the calibration phase.

Hereafter, we use the notation  $\hat{\pi}_T(\mathbf{x}) = \sigma_T(\mathbf{z}(\mathbf{x})) := \sigma(\mathbf{z}(\mathbf{x})/T)$  to denote the output of the softmax when taking into account the temperature. Observe that  $T = 1$  preserves the original probability vector. Since DNN classifiers are commonly overconfident, TS calibration typically yields

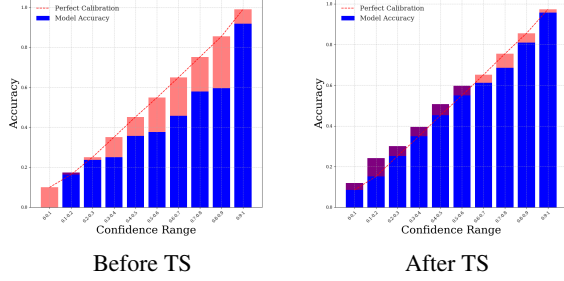


Figure 1. Reliability diagrams for ResNet50 trained on CIFAR-100 before and after TS calibration with ECE objective. The gap from slope of 1 (where the confidence matches the correctness probability) indicates the level of miscalibration.

some  $T > 1$ , which “softens” the original probability vector. Formally, TS with  $T > 1$  raises the entropy of the softmax output (see Proposition A.6 in the appendix).<sup>1</sup>

The *reliability diagram* (DeGroot & Fienberg, 1983; Niculescu-Mizil & Caruana, 2005) is a graphical depiction of a model before and after calibration. The confidence range  $[0, 1]$  is divided into bins and the validation samples (not used in the calibration) are assigned to the bins (according to  $\hat{\pi}_{\hat{y}(\mathbf{x})}(\mathbf{x})$ ). The average accuracy (Top-1) is computed per bin. In the case of perfect calibration, the diagram should be aligned with the identity function. Any significant deviation from slope of 1 indicates miscalibration. For example, the reliability diagram in Figure 1 shows the effectiveness of TS, based on ECE minimization, for calibrating a ResNet50 model trained on CIFAR-100 dataset.

## 2.2. Conformal Prediction

Conformal Prediction (CP) is a methodology that is model-agnostic and distribution-free, designed for generating a *prediction sets* of classes  $\mathcal{C}_\alpha(X)$  for a given sample  $X$ , such that  $Y \in \mathcal{C}_\alpha(X)$  with probability  $1 - \alpha$  (for a predefined  $\alpha \in (0, 1)$ ), where  $Y$  is the true class associated with  $X$  (Vovk et al., 1999; 2005; Papadopoulos et al., 2002). The decision rule is based on calibration set of labeled samples  $\{\mathbf{x}_i, y_i\}_{i=1}^n$ , which we hereafter refer to as the *CP set*, to avoid confusion with the set used for TS calibration. The only assumption in CP is that the random variables associated with the CP set and the test samples are exchangeable (e.g., the samples are i.i.d.).

Let us state the general process of conformal prediction given the CP set  $\{\mathbf{x}_i, y_i\}_{i=1}^n$  and its deployment for a new (test) sample  $x_{n+1}$  (for which  $y_{n+1}$  is unknown), as present

<sup>1</sup>We state and prove Proposition A.6 as we have not encountered such a result in the literature. Note increasing the entropy of  $\pi \in \Delta^{C-1}$  implies bringing it closer to uniform probability in the “Kullback-Leibler divergence” sense.

in (Angelopoulos & Bates, 2021):

1. Define a heuristic score function  $s(\mathbf{x}, y) \in \mathbb{R}$  based on some output of the model. A higher score should encode a lower level of agreement between  $\mathbf{x}$  and  $y$ .
2. Compute  $\hat{q}$  as the  $\frac{\lceil (n+1)(1-\alpha) \rceil}{n}$  quantile of the scores  $\{s(\mathbf{x}_1, y_1), \dots, s(\mathbf{x}_n, y_n)\}$ .
3. At deployment, use  $\hat{q}$  to create prediction sets for new examples:  $\mathcal{C}_\alpha(\mathbf{x}_{n+1}) = \{y : s(\mathbf{x}_{n+1}, y) \leq \hat{q}\}$ .

CP methods possess the following coverage guarantee.

**Theorem 2.1** (Theorem 1 in (Angelopoulos & Bates, 2021)). *Suppose that  $\{(X_i, Y_i)\}_{i=1}^n$  and  $(X_{n+1}, Y_{n+1})$  are i.i.d., and define  $\hat{q}$  as in step 2 above and  $\mathcal{C}_\alpha(X_{n+1})$  as in step 3 above. Then the following holds:*

$$\mathbb{P}(Y_{n+1} \in \mathcal{C}_\alpha(X_{n+1})) \geq 1 - \alpha. \quad (1)$$

The proof of this result is based on (Vovk et al., 1999). A proof of an upper bound of  $1 - \alpha + 1/(n+1)$  also exists. This property is called *marginal coverage* since the probability is taken over the entire distribution of  $(X, Y)$ . While achieving marginal coverage is practically feasible, it unfortunately *does not* imply the much more stringent concept of conditional coverage:

$$\mathbb{P}(Y_{n+1} \in \mathcal{C}_\alpha(X_{n+1}) | X_{n+1} = \mathbf{x}) \geq 1 - \alpha. \quad (2)$$

CP methods are usually compared by the size of their prediction sets, i.e., smaller  $\mathbb{E}[|\mathcal{C}_\alpha(X_{n+1})|]$  is better, and by their proximity to the conditional coverage property. Over time, various CP techniques with distinct objectives have been developed (Angelopoulos & Bates, 2021). There have been also efforts to alleviate the exchangeability assumption (Tibshirani et al., 2019; Barber et al., 2023).

In this paper we will focus on three prominent CP methods. Each of them devises a different score based on the output of the classifier’s softmax  $\hat{\pi}(\cdot)$ .

*Least Ambiguous Set-valued Classifier (LAC)* (Lei & Wasserman, 2014; Sadinle et al., 2019). In this method, the score is chosen to be  $s(\mathbf{x}, y) = 1 - \hat{\pi}_y(\mathbf{x})$ . Accordingly, given  $\hat{q}_{LAC}$  associated with  $\alpha$  through step 2, the prediction sets are formed as:  $\mathcal{C}^{LAC}(\mathbf{x}) := \{y : \hat{\pi}_y(\mathbf{x}) \geq 1 - \hat{q}_{LAC}\}$ . LAC tends to have small set sizes (under the strong assumption that  $\hat{\pi}_y(\mathbf{x})$  matches the posterior, it provably gives the smallest possible average set size). On the other hand, its conditional coverage is limited.

*Adaptive Prediction Sets (APS)* (Romano et al., 2020). The objective of this method is to improve the conditional coverage. Motivated by theory derived under the strong assumption that  $\hat{\pi}(\mathbf{x})$  matches the posterior probability, the

score is chosen to be  $s(\mathbf{x}, y) = \sum_{i=1}^{L_y} \hat{\pi}_{(i)}(\mathbf{x})$ , where  $\hat{\pi}_{(i)}(\mathbf{x})$

denotes the  $i$ -th element in a descendingly sorted version of  $\hat{\pi}(\mathbf{x})$  and  $L_y$  is the index that  $y$  is permuted to after sorting.

$\mathcal{C}^{APS}(\mathbf{x})$  includes  $\mathcal{C} = \{y : \sum_{i=1}^{L_y} \hat{\pi}_{(i)}(\mathbf{x}) \leq \hat{q}_{APS}\}$  and the class associated with  $\hat{\pi}_{(|\mathcal{C}|+1)}(\mathbf{x})$  to strictly ensure coverage, though typically this step undergoes randomization to match  $(1 - \alpha)$  coverage probability more precisely.

*Regularized Adaptive Prediction Sets (RAPS)* (Angelopoulos et al., 2021). A modification of APS that aims at improving its prediction sets sizes by penalizing hard examples to reduce their effect on  $\hat{q}$ . This comes with some compromise on the improvement in conditional coverage. With the same notation as APS, in RAPS we have

$s(\mathbf{x}, y) = \sum_{i=1}^{L_y} \hat{\pi}_{(i)}(\mathbf{x}) + \lambda(L_y - k_{reg})_+$ , where  $\lambda, k_{reg} \geq 0$

are regularization hyperparameters.  $\mathcal{C}^{RAPS}(\mathbf{x})$  includes  $\mathcal{C} = \{y : \sum_{i=1}^{L_y} \hat{\pi}_{(i)}(x) + \lambda(L_y - k_{reg})_+ \leq \hat{q}_{RAPS}\}$  and,

typically under some randomization, the class associated with  $\hat{\pi}_{(|\mathcal{C}|+1)}(\mathbf{x})$ , similarly to APS.

Note that all these CP methods can be readily applied on  $\pi_T(\cdot)$  after TS (or other traditional calibration). This is done, e.g., in (Angelopoulos et al., 2021). However, neither (Angelopoulos et al., 2021) nor any other work examined the effect that TS (or calibration in general) has on any CP method.

### 3. The Effect of Temperature Scaling on CP Methods for DNN Classifiers

In this section, we empirically investigate the effect of TS on the performance of CP algorithms. Specifically, we consider different datasets and models, and start by reporting the mean prediction set size and coverage of CP algorithms, with and without an initial TS calibration procedure. Then, we discuss the results and gain more empirical insights by examining various metrics for different values of the temperature  $T$  (beyond the effect of the value of  $T$  that is optimal for calibration).

#### 3.1. Experimental setup

The models and datasets utilized in the experiments are as follows.

**Datasets.** To investigate the effect, we conducted our experiment on CIFAR-10, CIFAR-100 (Krizhevsky et al., 2009) and ImageNet (Deng et al., 2009) chosen for their diverse content and varying levels of difficulty.

**Models.** We utilized a diverse set of DNN classifiers, based on ResNets (He et al., 2016) and DenseNets (Huang et al., 2017). For CIFAR-10: ResNet34 and ResNet50. For CIFAR-100: ResNet50 and DenseNet121. For ImageNet: ResNet152 and DenseNet121.

**TS calibration.** For each of the dataset-model pairs, we determine the optimal temperature by constructing a calibration set by randomly selecting 20% of the validation set, and optimizing the temperature  $T$  by minimizing the ECE.

**CP Algorithms.** For each of the dataset-model pairs, we construct the ‘‘CP set’’ (used for computing the thresholds of CP methods) by randomly selecting 20% of the validation set, while ensuring not to include in the CP set samples that are used in the TS calibration. The CP methods that we examine are LAC, APS, and RAPS, detailed in Section 2.2 (we use the randomized versions of APS and RAPS, as done in (Angelopoulos et al., 2021)). For each technique, we use  $\alpha = 0.1$ , so the desired marginal coverage probability is  $1 - \alpha = 0.9$ , as common in most CP literature (Romano et al., 2020; Angelopoulos et al., 2021; Angelopoulos & Bates, 2021).

**Metrics.** We report several metrics that are averaged over 60% of the validation samples that have not been included in the calibration and CP sets. In addition to the popular Top-1 and Top-5 accuracy metrics (which are independent of TS and CP), we report the mean prediction set size and the mean marginal coverage, computed as the empirical mean of  $\mathbb{I}\{Y^{(val)} \in C(X^{(val)})\}$ . Additionally, as a metric that can reflect conditional coverage, we use

$$\min_{g \in \{1, \dots, G\}} \frac{1}{|I_g|} \sum_{i \in I_g} \mathbb{I}\{Y_i^{(val)} \in C(X_i^{(val)})\}.$$

This metric returns the minimum coverage among  $G$  different groups of the validation data, where  $I_g \subset \{1, \dots, n_{val}\}$  includes the indexes of the samples belonging to group  $g$ . For simplicity, we choose each group to be a class in the considered dataset.

We iterate through this procedure (which includes the selection of the calibration and CP sets) over 100 trials and calculate the median-of-means for both coverage metrics and prediction set size.

#### 3.2. Results: accuracy, coverage and prediction set size

For each of the dataset-model pairs we compute the aforementioned metrics with and without an initial TS calibration procedure. In Table 1, we report the the optimal temperature  $T$ , the accuracy (which is not affected by TS), and the median-of-means of prediction sets sizes. In Tables 2 and 3, we report the marginal and conditional coverage results, respectively.

Table 1. Mean prediction set size with and without initial TS, along with accuracy and optimal  $T$ .

| Dataset-Model          | Optimal $T$ | Accuracy |       | Mean set size |      |      | Mean set size after TS |      |      |
|------------------------|-------------|----------|-------|---------------|------|------|------------------------|------|------|
|                        |             | Top-1    | Top-5 | LAC           | APS  | RAPS | LAC                    | APS  | RAPS |
| CIFAR-100, ResNet50    | 1.524       | 0.809    | 0.954 | 1.62          | 5.35 | 2.68 | 1.57                   | 9.34 | 4.96 |
| CIFAR-100, DenseNet121 | 1.469       | 0.761    | 0.935 | 2.13          | 4.36 | 2.95 | 2.06                   | 6.81 | 4.37 |
| ImageNet, ResNet152    | 1.227       | 0.783    | 0.940 | 1.95          | 7.34 | 3.30 | 1.92                   | 12.5 | 4.40 |
| ImageNet, DenseNet121  | 1.024       | 0.744    | 0.919 | 2.73          | 13.1 | 4.70 | 2.76                   | 13.3 | 4.88 |
| CIFAR-10, ResNet50     | 1.761       | 0.946    | 0.997 | 0.91          | 1.04 | 0.98 | 0.91                   | 1.13 | 1.05 |
| CIFAR-10, ResNet34     | 1.802       | 0.953    | 0.998 | 0.91          | 1.03 | 0.94 | 0.93                   | 1.11 | 1.05 |

Table 2. Marginal coverage with and without initial TS.

| Dataset-Model    | Coverage |       |       | Coverage after TS |       |       |
|------------------|----------|-------|-------|-------------------|-------|-------|
|                  | LAC      | APS   | RAPS  | LAC               | APS   | RAPS  |
| CIFAR-100, RN50  | 0.901    | 0.928 | 0.899 | 0.902             | 0.959 | 0.900 |
| CIFAR-100, DN121 | 0.900    | 0.918 | 0.899 | 0.900             | 0.941 | 0.900 |
| ImageNet, RN152  | 0.899    | 0.925 | 0.900 | 0.899             | 0.937 | 0.900 |
| ImageNet, DN121  | 0.900    | 0.924 | 0.899 | 0.900             | 0.925 | 0.899 |
| CIFAR-10, RN50   | 0.900    | 0.958 | 0.900 | 0.899             | 0.966 | 0.900 |
| CIFAR-10, RN34   | 0.900    | 0.964 | 0.899 | 0.900             | 0.972 | 0.900 |

Table 3. Minimal class coverage with and without initial TS.

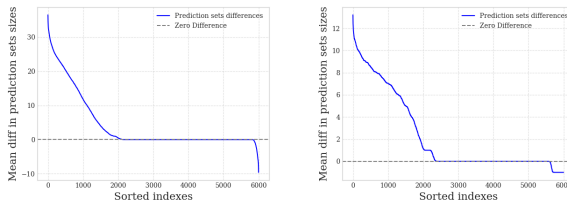
| Dataset-Model    | Min class coverage |       |       | Min class cov. after TS |       |       |
|------------------|--------------------|-------|-------|-------------------------|-------|-------|
|                  | LAC                | APS   | RAPS  | LAC                     | APS   | RAPS  |
| CIFAR-100, RN50  | 0.696              | 0.780 | 0.765 | 0.750                   | 0.831 | 0.797 |
| CIFAR-100, DN121 | 0.774              | 0.785 | 0.795 | 0.753                   | 0.839 | 0.805 |
| ImageNet, RN152  | 0.441              | 0.613 | 0.540 | 0.421                   | 0.644 | 0.621 |
| ImageNet, DN121  | 0.447              | 0.555 | 0.542 | 0.441                   | 0.558 | 0.555 |
| CIFAR-10, RN50   | 0.788              | 0.905 | 0.852 | 0.787                   | 0.922 | 0.867 |
| CIFAR-10, RN34   | 0.809              | 0.932 | 0.871 | 0.810                   | 0.942 | 0.875 |

We remark that all the optimal temperatures in Table 1 are greater than 1, indicating that the models exhibit overconfidence. The reliability diagrams for ResNet50 trained on CIFAR-100 before and after TS calibration are presented in Figure 1. In Appendix B.3, we present the reliability diagrams for the other dataset-model pairs. For completeness, we also report there the optimal temperatures when the calibration objective is NLL, which resemble the results when optimizing ECE (all of them are still greater than 1).

### 3.3. Discussion and more empirical insights

From Table 2, we see that all the CP methods possess marginal coverage with and without an initial TS procedure, which is aligned with CP theoretical guarantees (Theorem 2.1). In general, the TS neither harms nor improves this property.

As for the conditional coverage, reflected here by the minimal per-class coverage, we see from Table 3 that LAC has conditional coverage which is not affected by the TS in most cases, and it inferior to APS and RAPS. APS has the best conditional coverage. The conditional coverage of both APS and RAPS increases when the TS is applied. Yet, the improvement is rather minor.



CIFAR-100, ResNet50, APS    CIFAR-100, ResNet50, RAPS

Figure 2. Mean sorted differences in prediction sets sizes with and without initial TS calibration. Observe that the calibration has an overall negative impact on the prediction sets sizes (more samples exhibit an increase in the set size than a decrease, and the extent of the increase is greater).

The most thought provoking observations come from Table 1, which reports the effect of TS on the prediction set size of the CP methods. First, we see that the effect of TS on LAC is negligible. Second, we see that for the models trained on CIFAR-10, whose Top-1 accuracy is higher than the desired  $1 - \alpha = 0.9$  coverage, the effect of TS is also negligible. Third, for the other models (which are less accurate than  $1 - \alpha$ ) we see that the TS procedure has led to *increase* in the mean prediction set size for APS and RAPS. Especially, when the value of the optimal  $T$  is high. For example, for ResNet50 trained on CIFAR-100, the TS calibration increases the mean prediction set size of APS from 5.35 to 9.34.

The last observation is quite surprising. Why would a procedure like TS, which improves the alignment of the post-softmax dominant bin with the true marginal correctness probability, have a detrimental effect on the length of the sets required for marginal coverage of the adaptive CP methods APS and RAPS?

To verify that the increase in the mean set size for APS and RAPS is not caused by a small number of extreme outliers, we “microscopically” analyze the change per sample. Specifically, for each sample in the validation set, we compare the prediction set size after the CP procedure with and without the initial TS calibration (i.e., set size with TS minus set size without TS). Sorting the differences in a descending

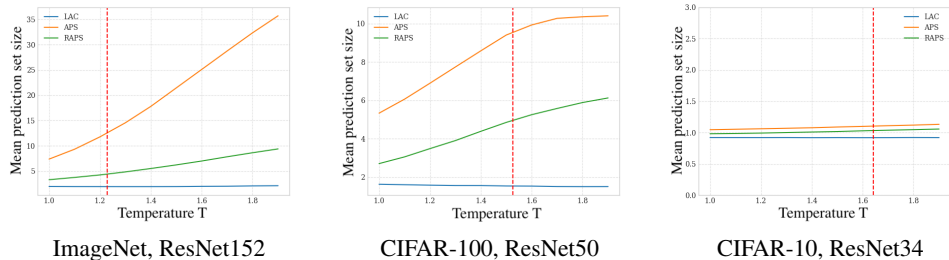


Figure 3. Mean prediction set size for LAC, APS and RAPS versus the temperature  $T$ .

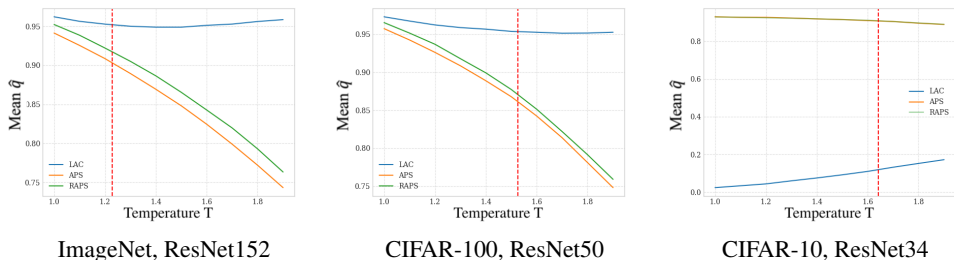


Figure 4. Mean threshold  $\hat{q}$  for LAC, APS and RAPS versus the temperature  $T$ .

order yields a staircase-shaped curve. The smoothed version of this curve, which is obtained after averaging over the 100 trials (random selections of calibration and CP sets), is presented in Figure 2 for ResNet50 trained on CIFAR-10, both for APS and for RAPS.

In the experiment depicted in Figure 2, approximately one-third of the samples experience a negative impact on the prediction set size due to the TS procedure. For about half of the samples, there is no change in set size. Only for the remaining small minority of samples, TS provided some assistance but to a much lesser extent than the harm observed for others. Similar behavior is observed for other dataset-model pairs, as displayed by the figures in Appendix B.

Below, in Section 4, we aim to provide mathematical reasoning for the overall negative effect of TS (with  $T > 1$ ) on the prediction set size of APS and RAPS. Interestingly, the existence of samples (though few) where the TS procedure causes a decrease in set size indicates that we cannot make a universal (uniform) statement about the impact of TS on the set size of arbitrary sample.

Lastly, we turn to gain empirical insights of the effect of values of  $T$  on CP techniques, beyond the value that is optimal for calibration. Specifically, we examine the mean prediction sets sizes, as well as the threshold value  $\hat{q}$ , of LAC, APS, and RAPS, for values of  $T$  ranging from 1 to 2 with an increment of 0.1. The results for various dataset-model pairs are presented in Figures 3 and 4, where the red dashed vertical line marks the optimal  $T$  for calibration.

For ImageNet and CIFAR-100 datasets, and for APS and RAPS algorithms, we see a significant increase in the mean prediction set size along with decrease in the threshold value  $\hat{q}$  as  $T$  increases. These observations imply that a theoretical analysis need not restrict itself to the optimal  $T$  but rather examine more general  $T > 1$ . Furthermore, note that a decrease in the threshold  $\hat{q}$  does not necessarily lead to larger prediction sets. A naive example is reducing  $\hat{q}$  simply by defining a modified CP score where some constant is subtracted from  $s(\mathbf{x}, y)$ . This hints that the empirical behavior observed in this section is due to effect of TS on APS and RAPS scores that depends on the sample’s logits (or roughly, whether it is hard or easy).

To conclude, in this section we established the following empirical observations, which will be considered in the following theoretical section.

**Observation 1.** The effect of TS on the performance of CP algorithms is minor for “very accurate” models, whose Top-1 accuracy is significantly greater than  $1 - \alpha$ .

**Observation 2.** Increasing the temperature monotonically reduces the threshold of APS and RAPS.

**Observation 3.** For “less accurate” models, increasing the temperature oftentimes increases the size of the prediction sets produced by APS and RAPS.

In addition, we observed that TS has a negligible effect on LAC, and slightly improves the conditional coverage property of APS and RAPS. Yet, we leave the theoretical analysis of these two additional observations for future research.

## 4. Theoretical Analysis

In this section, we provide mathematical reasoning for observations stated in Section 3.3. *All the proofs are provided in Appendix A.*

### 4.1. TS affects coverage only through misclassified samples

Observation 1 states that the effect of TS (even with rather large  $T$ ) on CP methods' performance is negligible in "easy" settings where the models' Top-1 accuracy is significantly above  $1 - \alpha$ . Indeed, in such cases it is enough to pick the single class that dominates the softmax in order to achieve coverage. In the following proposition we generalize this behavior, showing that *in general* (not only for models that are "accurate enough") TS affects the coverage of CP methods only through misclassified samples.

**Proposition 4.1.** *Let  $\hat{y}(x)$  estimate the class according to the dominant entry in the post-softmax vector. Assume that a CP method uses a score that preserves the ranking of the post-softmax vector (the common case). Then, TS affects the coverage property the CP method (Eq. (1)) only through samples that are misclassified.*

This proposition can be generalized to coverage conditioned on groups, which further motivates separating the data into domains with different classification difficulty and applying CP separately.

### 4.2. TS decreases the threshold of APS and RAPS

Observation 2 states that increasing the temperature monotonically reduces the threshold of APS and RAPS. We will prove this theoretically.

Recall the score in the APS method  $s(\mathbf{x}, y) = \sum_{i=1}^{L_y} \hat{\pi}_{(i)}(\mathbf{x})$ ,

where  $\hat{\pi}_{(i)}(\mathbf{x})$  denotes the  $i$ -th element in a descendingly sorted version of  $\hat{\pi}(\mathbf{x})$  and  $L_y$  is the index that  $y$  is permuted to after sorting. Recall that the RAPS algorithm is based on the same score with an additional regularization term that is not affected by TS. Let us denote by  $s_T(\mathbf{x}, y)$  the score of the same sample after TS, i.e., using  $\hat{\pi}_T(\mathbf{x})$ . Note that

$$s_T(\mathbf{x}, y) = \sum_{i=1}^{L_y} \hat{\pi}_{T,(i)}(\mathbf{x}) = \sum_{i=1}^{L_y} [\sigma(\ln(\hat{\pi}(\mathbf{x}))/T)]_{(i)}$$

where we use the fact that  $\hat{\pi}_T = \sigma(\ln(\hat{\pi})/T)$ , which follows from the ability to recover the logits  $\mathbf{z}(\mathbf{x}) = \ln(\hat{\pi}(\mathbf{x}))$  up to a constant  $c\mathbf{1}_C$ , which does not affect the softmax also after scaling by  $T$ . Here,  $\ln(\cdot)$  operates entry-wise. In addition, note that TS does not change the ranking of the entries.

We now state a theorem that shows that TS with  $T > 1$

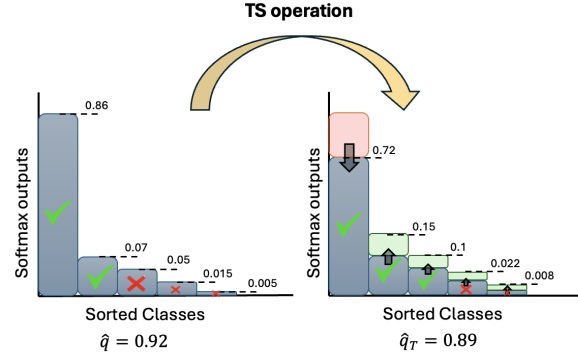


Figure 5. Illustration of the typical effect of TS on the softmax output. In the experiments that we conducted, TS (with  $T > 1$ ) typically decreases the value only in the most dominant bin, causing an increase in the values of the other bins. The figure provides an example for a specific setting (distribution and threshold values) where the prediction set size without TS is 2, but with TS, it becomes 3. With the notations of Section 4, we have  $L = 2$  and it

holds that  $\sum_{j=1}^L \hat{\pi}_j - \sum_{j=1}^L \hat{\pi}_{T,j} > \hat{q} - \hat{q}_T$ .

decreases the cumulative sum of sorted probability vectors, akin to the score used by APS.

**Theorem 4.2.** *Let  $\pi \in \Delta^{C-1}$  (probability vector in  $\mathbb{R}^C$ ) such that  $\pi_1 \geq \pi_2 \geq \dots \geq \pi_C$  (i.e., sorted) and let  $T \geq 1$  and  $L \in [C]$ . Then, we have*

$$\sum_{j=1}^L \pi_j \geq \sum_{j=1}^L \pi_{T,j},$$

where  $\pi_T = \sigma(\ln(\pi)/T)$  is the softmax output after applying TS with  $T$  on the logits associated with  $\pi$ . The inequality is strict, unless  $L = C$  or  $T = 1$  or  $\pi_1 = \dots = \pi_C$ .

Note that Theorem 4.2 is universal: it holds for any sorted probability vector. Denote the threshold obtained by applying the CP method after TS by  $\hat{q}_T$ . Based on the universality of the theorem, we can establish the that increasing the temperature  $T$  decreases  $\hat{q}_T$  for APS and RAPS.

**Corollary 4.3.** *The threshold value  $\hat{q}_T$  of the non-randomized version of APS and RAPS decreases monotonically as the temperature  $T$  increases above 1.*

To simplify the arguments (and avoid pathological random cases), the corollary is stated for APS and RAPS without their randomized modification. Under the realistic assumption that the samples in the CP set do not satisfy the conditions that turn the inequality into equality in Theorem 4.2, it is not hard to turn the statement into strict decrease of  $\hat{q}_T$ .

### 4.3. TS tends to increase the prediction set size of APS

Observation 3 in Section 3.3 states that (empirically) increasing the temperature many times increases the size of

the prediction sets produced by APS and RAPS. For simplification we consider here the plain (non-randomized) APS.

Formally, for a new test sample  $\mathbf{x}$  (not from calibration or CP sets) denote by  $\hat{\boldsymbol{\pi}}$  and  $\hat{\boldsymbol{\pi}}_T$  the softmax output with and without TS, respectively, *after being sorted* in descending order. (The relation  $\hat{\boldsymbol{\pi}}_T = \boldsymbol{\sigma}(\ln(\hat{\boldsymbol{\pi}})/T)$  still holds.) We

have that  $L = \min\{l : \sum_{i=1}^l \hat{\pi}_i \geq \hat{q}\}$ ,  $L_T = \min\{l :$

$\sum_{i=1}^l \hat{\pi}_{T,i} \geq \hat{q}_T\}$  are the prediction set sizes for this sample

according to APS with and without TS, respectively. Our experiments show that  $L_T \geq L$  for “typical”  $\mathbf{x}$ . Namely, in the practical settings that we examined it is more likely that this inequality holds than that it does not. See Figure 5 for illustration.

Alternatively, we can study the event

$$\sum_{i=1}^L \hat{\pi}_i - \sum_{i=1}^L \hat{\pi}_{T,i} \geq \hat{q} - \hat{q}_T, \quad (3)$$

as shown in Proposition A.5 (which uses  $\hat{q} \geq \hat{q}_T$  ensured by Corollary 4.3). Namely, TS (with  $T > 1$ ) affects “typical” samples more than it affects the samples (in the CP set) that determine the thresholds  $\hat{q}, \hat{q}_T$ . Since  $1 - \alpha$  is large, the samples that determine  $\hat{q}, \hat{q}_T$  are expected to be harder for classification, e.g., without a dominant entry in their post-softmax vectors.

To further simplify the problem, let us assume that both  $\hat{q}, \hat{q}_T$  are associated with the same sample in the CP set,  $\mathbf{x}^{hard}$ , for which we can associate the (sorted) softmax outputs  $\boldsymbol{\pi}^{hard}$  and  $\boldsymbol{\pi}_T^{hard} = \boldsymbol{\sigma}(\ln(\boldsymbol{\pi}^{hard})/T)$ . With this assumption, we see that studying (3) translates to studying the “gap function”

$$g(\boldsymbol{\pi}; T, L) = \sum_{i=1}^L \pi_i - \sum_{i=1}^L \sigma_i\left(\frac{1}{T} \ln \boldsymbol{\pi}\right) \quad (4)$$

showing that  $g(\hat{\boldsymbol{\pi}}; T, L) \geq g(\boldsymbol{\pi}^{hard}; T, L^{hard})$ . Note that Theorem 4.2 already teaches us that  $g(\boldsymbol{\pi}; T, L) \geq 0$  for  $T \geq 1$ . However, precise global analysis of  $g(\boldsymbol{\pi}; T, L)$  appears to be very challenging. Therefore, we turn to use a local analysis.

Since  $\boldsymbol{\pi}^{hard}$  is more dispersed (less decisive) than a “typical”  $\hat{\boldsymbol{\pi}}$ , which tend to have a dominant first entry, for the analysis we model  $\hat{\boldsymbol{\pi}} - \boldsymbol{\pi}^{hard}$  by a prototypical vector  $\mathbf{r}$  with a dominant first entry (and such that with small enough  $\|\mathbf{r}\|$ ,  $\boldsymbol{\pi}^{hard} + \mathbf{r}$  is still in  $\Delta^{C-1}$ ). The following theorem establishes a connection between the derivative of  $g(\boldsymbol{\pi}; T, L)$  in the direction of  $\mathbf{r}$  and the value of  $T$  that ensures that  $\mathbf{r}$  is an ascent direction.

**Theorem 4.4.** *Let  $\boldsymbol{\pi} \in \Delta^{C-1}$  be a probability vector with*

*$\pi_i > 0$ , and mean  $\bar{\pi} = \frac{1}{C} \sum_{i=1}^C \pi_i$ . Let  $L \in [C - 1]$  and*

*$\mathbf{r} = [\delta, -\frac{1}{C-1}\delta, \dots, -\frac{1}{C-1}\delta]^\top$  with some  $\delta > 0$ . If*

$$T > \frac{C\sqrt{L}}{(C-L)\pi_1} + \frac{\sqrt{L}}{(C-L)} \left\| [\pi_1^{-1} - \bar{\pi}^{-1}, \dots, \pi_C^{-1} - \bar{\pi}^{-1}] \right\|_2,$$

*then  $g(\boldsymbol{\pi}; T, L)$  stated in (4) obeys*

$$\mathbf{r}^\top \nabla_{\boldsymbol{\pi}} g(\boldsymbol{\pi}; T, L) > 0.$$

While Theorem 4.4 holds for quite general  $\boldsymbol{\pi} \in \Delta^{C-1}$ , inspecting the effect of  $\boldsymbol{\pi}$  on lower bound on  $T$  provides some insights. In particular, we see that the second term in the bound decreases as  $\boldsymbol{\pi}$  is closer to the center of the simplex (uniform probability), which can be interpreted as being associated with a hard sample. Thus, in such case, even rather small  $T$  suffices for increasing  $g$  when taking a step toward the dominant vertex. Note that  $\mathbf{r}$  stated in the theorem is chosen to simplify the analysis, but the statement can be generalized to other instances of  $\mathbf{r}$  with dominant first entry.

Even though Theorem 4.4 presents a local analysis of  $g(\cdot; T, L)$ , it provides a formal reasoning why it is likely that  $g(\hat{\boldsymbol{\pi}}; T, L) > g(\boldsymbol{\pi}^{hard}; T, L)$ . Adding to this the reasonable assumption that  $g(\boldsymbol{\pi}^{hard}; T, L) > g(\boldsymbol{\pi}^{hard}; T, L^{hard})$  due to  $g(\boldsymbol{\pi}^{hard}; T, L^{hard})$  summing over  $L^{hard} - L > 0$  additional negative entries of  $\boldsymbol{\pi}^{hard} - \boldsymbol{\pi}_T^{hard}$  (recall Figure 5), further explains having  $g(\hat{\boldsymbol{\pi}}; T, L) > g(\boldsymbol{\pi}^{hard}; T, L^{hard})$ .

## 5. Conclusion

In this work, we studied the effect the widely used temperature scaling (TS) calibration on the performance of conformal prediction (CP) techniques. These popular complementary approaches are useful for assessing the reliability of classifiers, in particular those that are based DNNs. Yet, their interplay has not been examined so far. We conducted an extensive empirical study, which revealed that initial TS calibration affects CP methods differently. Surprisingly, it tends to have a detrimental effect on the prediction sets sizes of the adaptive CP methods (APS and RAPS). We theoretically studied the tension between TS and the procedures of APS and RAPS, gaining some insights on the behavior.

Our work challenges the common practice of calibrating DNNs before applying other post-processing algorithms. In particular, for overconfident models, it suggests basing adaptive CP methods (chosen for their enhanced conditional coverage) on softmax values before temperature scaling or after canceling it. We hope that this paper will motivate future research on the interplay between different calibration and CP techniques.

**Acknowledgment.** The work is supported by ISF grant 1940/23.



## References

- Angelopoulos, A. N. and Bates, S. A gentle introduction to conformal prediction and distribution-free uncertainty quantification. *arXiv preprint arXiv:2107.07511*, 2021.
- Angelopoulos, A. N., Bates, S., Jordan, M., and Malik, J. Uncertainty sets for image classifiers using conformal prediction. In *International Conference on Learning Representations*, 2021.
- Barber, R. F., Candes, E. J., Ramdas, A., and Tibshirani, R. J. Conformal prediction beyond exchangeability. *The Annals of Statistics*, 51(2):816–845, 2023.
- Cosmides, L. and Tooby, J. Are humans good intuitive statisticians after all? rethinking some conclusions from the literature on judgment under uncertainty. *cognition*, 58(1):1–73, 1996.
- DeGroot, M. H. and Fienberg, S. E. The comparison and evaluation of forecasters. *Journal of the Royal Statistical Society: Series D (The Statistician)*, 32(1-2):12–22, 1983.
- Deng, J., Dong, W., Socher, R., Li, L.-J., Li, K., and Fei-Fei, L. Imagenet: A large-scale hierarchical image database. In *2009 IEEE conference on computer vision and pattern recognition*, pp. 248–255. Ieee, 2009.
- Ding, Z., Han, X., Liu, P., and Niethammer, M. Local temperature scaling for probability calibration. In *Proceedings of the IEEE/CVF International Conference on Computer Vision*, pp. 6889–6899, 2021.
- Frenkel, L. and Goldberger, J. Network calibration by class-based temperature scaling. In *2021 29th European Signal Processing Conference (EUSIPCO)*, pp. 1486–1490. IEEE, 2021.
- Grigorescu, S., Trasnea, B., Cocias, T., and Macesanu, G. A survey of deep learning techniques for autonomous driving. *Journal of Field Robotics*, 37(3):362–386, 2020.
- Guo, C., Pleiss, G., Sun, Y., and Weinberger, K. Q. On calibration of modern neural networks. In *International conference on machine learning*, pp. 1321–1330. PMLR, 2017.
- Guo, W., Mu, D., Xu, J., Su, P., Wang, G., and Xing, X. Lemna: Explaining deep learning based security applications. In *proceedings of the 2018 ACM SIGSAC conference on computer and communications security*, pp. 364–379, 2018.
- Hastie, T., Tibshirani, R., Friedman, J., and Franklin, J. The elements of statistical learning: data mining, inference and prediction. *The Mathematical Intelligencer*, 27(2): 83–85, 2005.
- He, K., Zhang, X., Ren, S., and Sun, J. Deep residual learning for image recognition. In *Proceedings of the IEEE conference on computer vision and pattern recognition*, pp. 770–778, 2016.
- Huang, G., Liu, Z., Van Der Maaten, L., and Weinberger, K. Q. Densely connected convolutional networks. In *Proceedings of the IEEE conference on computer vision and pattern recognition*, pp. 4700–4708, 2017.
- Ji, B., Jung, H., Yoon, J., Kim, K., et al. Bin-wise temperature scaling (bts): Improvement in confidence calibration performance through simple scaling techniques. In *2019 IEEE/CVF International Conference on Computer Vision Workshop (ICCVW)*, pp. 4190–4196. IEEE, 2019.
- Krizhevsky, A., Hinton, G., et al. Learning multiple layers of features from tiny images. 2009.
- Krizhevsky, A., Sutskever, I., and Hinton, G. E. Imagenet classification with deep convolutional neural networks. *Advances in neural information processing systems*, 25, 2012.
- Lei, J. and Wasserman, L. Distribution-free prediction bands for non-parametric regression. *Journal of the Royal Statistical Society Series B: Statistical Methodology*, 76(1): 71–96, 2014.
- Liang, S., Li, Y., and Srikant, R. Enhancing the reliability of out-of-distribution image detection in neural networks. In *International Conference on Learning Representations*, 2018.
- Miotto, R., Wang, F., Wang, S., Jiang, X., and Dudley, J. T. Deep learning for healthcare: review, opportunities and challenges. *Briefings in bioinformatics*, 19(6):1236–1246, 2018.
- Naeini, M. P., Cooper, G., and Hauskrecht, M. Obtaining well calibrated probabilities using bayesian binning. In *Proceedings of the AAAI conference on artificial intelligence*, volume 29, 2015.
- Niculescu-Mizil, A. and Caruana, R. Predicting good probabilities with supervised learning. In *Proceedings of the 22nd international conference on Machine learning*, pp. 625–632, 2005.
- Nixon, J., Dusenberry, M. W., Zhang, L., Jerfel, G., and Tran, D. Measuring calibration in deep learning. In *CVPR workshops*, volume 2, 2019.
- Papadopoulos, H., Proedrou, K., Vovk, V., and Gammerman, A. Inductive confidence machines for regression. In *Machine Learning: ECML 2002: 13th European Conference on Machine Learning Helsinki, Finland, August 19–23, 2002 Proceedings 13*, pp. 345–356. Springer, 2002.

- Platt, J. et al. Probabilistic outputs for support vector machines and comparisons to regularized likelihood methods. *Advances in large margin classifiers*, 10(3):61–74, 1999.
- Romano, Y., Sesia, M., and Candes, E. Classification with valid and adaptive coverage. *Advances in Neural Information Processing Systems*, 33:3581–3591, 2020.
- Sadinle, M., Lei, J., and Wasserman, L. Least ambiguous set-valued classifiers with bounded error levels. *Journal of the American Statistical Association*, 114(525):223–234, 2019.
- Tibshirani, R. J., Foygel Barber, R., Candes, E., and Ramdas, A. Conformal prediction under covariate shift. *Advances in neural information processing systems*, 32, 2019.
- Vovk, V., Gammerman, A., and Saunders, C. Machine-learning applications of algorithmic randomness. In *Proceedings of the Sixteenth International Conference on Machine Learning*, pp. 444–453, 1999.
- Vovk, V., Gammerman, A., and Shafer, G. *Algorithmic learning in a random world*, volume 29. Springer, 2005.
- Wang, D.-B., Feng, L., and Zhang, M.-L. Rethinking calibration of deep neural networks: Do not be afraid of overconfidence. *Advances in Neural Information Processing Systems*, 34:11809–11820, 2021.
- Wei, H., Xie, R., Cheng, H., Feng, L., An, B., and Li, Y. Mitigating neural network overconfidence with logit normalization. In *International Conference on Machine Learning*, pp. 23631–23644. PMLR, 2022.
- Zadrozny, B. and Elkan, C. Transforming classifier scores into accurate multiclass probability estimates. In *Proceedings of the eighth ACM SIGKDD international conference on Knowledge discovery and data mining*, pp. 694–699, 2002.

## A. Proofs.

**Proposition A.1.** *Let  $\hat{y}(x)$  estimate the class according to the dominant entry in the post-softmax vector. Assume that a CP method uses a score that preserves the ranking of the post-softmax vector (the common case). Then, TS affects the coverage property the CP method (Eq. (1)) only through samples that are misclassified.*

*Proof.* The proof utilizes the law of total expectation (note that  $\mathbb{P}(Y \in \mathcal{C}_\alpha(X)) = \mathbb{E}[\mathbb{I}\{Y \in \mathcal{C}_\alpha(X)\}]$ ).

We have

$$\begin{aligned} \mathbb{P}(Y \in \mathcal{C}_\alpha(X)) &= \int p_X(x) \mathbb{P}(Y \in \mathcal{C}_\alpha(X) | X = x) dx \\ &= \int p_X(x) \left[ \mathbb{P}(\hat{y}(X) = Y | X = x) \mathbb{P}(Y \in \mathcal{C}_\alpha(X) | X = x, \hat{y}(X) = Y) \right. \\ &\quad \left. + \mathbb{P}(\hat{y}(X) \neq Y | X = x) \mathbb{P}(Y \in \mathcal{C}_\alpha(X) | X = x, \hat{y}(X) \neq Y) \right] dx. \end{aligned} \quad (5)$$

Now, observe that TS does not change the predicted class, Thus, it *does not* change  $\mathbb{P}(\hat{y}(X) = Y | X = x)$  and  $\mathbb{P}(\hat{y}(X) \neq Y | X = x)$ . Moreover, since the CP method preserves the ranking of the post-softmax vector we have  $\mathbb{P}(Y \in \mathcal{C}_\alpha(X) | X = x, \hat{y}(X) = Y) = 1$ . Therefore, the only expression in (5) that is affected by TS is  $\mathbb{P}(Y \in \mathcal{C}_\alpha(X) | X = x, \hat{y}(X) \neq Y)$ , which considers only the misclassification event.  $\square$

**Theorem A.2.** *Let  $\pi \in \Delta^{C-1}$  (probability vector in  $\mathbb{R}^C$ ) such that  $\pi_1 \geq \pi_2 \geq \dots \geq \pi_C$  (i.e., sorted) and let  $T \geq 1$  and  $L \in [C]$ . Then, we have*

$$\sum_{j=1}^L \pi_j \geq \sum_{j=1}^L \pi_{T,j},$$

where  $\pi_T = \sigma(\ln(\pi)/T)$  is the softmax output after applying TS with  $T$  on the logits associated with  $\pi$ . The inequality is strict, unless  $L = C$  or  $T = 1$  or  $\pi_1 = \dots = \pi_C$ .

*Proof.* The statement, which is given in the “probability domain”  $\pi \in \Delta^{C-1}$ , can be equivalently stated for logits  $\mathbf{z} \in \mathbb{R}^C$ . The reason is that the softmax does no change the ranking and is invertible up to a constant  $\sigma(\ln \pi + c\mathbf{1}_C) = \pi$ .

**Theorem.** *Let  $\mathbf{z} \in \mathbb{R}^C$  such that  $z_1 \geq z_2 \geq \dots \geq z_C$  (i.e., sorted) and let  $T \geq 1$  and  $L \in [C]$ . Then, we have*

$$\sum_{j=1}^L \frac{\exp(z_j)}{\sum_{c=1}^C \exp(z_c)} \geq \sum_{j=1}^L \frac{\exp(z_j/T)}{\sum_{c=1}^C \exp(z_c/T)}. \quad (6)$$

The inequality is strict, unless  $T = 1$  or  $z_1 = \dots = z_C$ .

Before we turn to prove the theorem, let us prove an auxiliary lemma.

**Lemma.** *Let  $z_i, z_j \in \mathbb{R}$  such that  $z_i \geq z_j$  and let  $T \geq 1$ . Then, the following holds*

$$\exp(z_i) \cdot \exp(z_j/T) \geq \exp(z_i/T) \cdot \exp(z_j).$$

The inequality is strict, unless  $T = 1$  or  $z_i = z_j$ .

*Proof.* Since  $z_i - z_j \geq 0$  and  $1 - 1/T \geq 0$  we have that

$$\exp \left[ (z_i - z_j) \left( 1 - \frac{1}{T} \right) \right] \geq 1,$$

where the inequality is strict, unless  $T = 1$  or  $z_i = z_j$ . Next, observe that

$$\begin{aligned} \exp \left[ (z_i - z_j) \left( 1 - \frac{1}{T} \right) \right] &= \exp \left[ z_i \left( 1 - \frac{1}{T} \right) - z_j \left( 1 - \frac{1}{T} \right) \right] \\ &= \frac{\exp \left( z_i + \frac{z_j}{T} \right)}{\exp \left( \frac{z_i}{T} + z_j \right)} \\ &= \frac{\exp(z_i) \cdot \exp(z_j/T)}{\exp(z_i/T) \cdot \exp(z_j)}. \end{aligned}$$

Using the inequality we have  $\frac{\exp(z_i) \cdot \exp(z_j/T)}{\exp(z_i/T) \cdot \exp(z_j)} \geq 1$ , which concludes the proof of the lemma.  $\square$

### Back to the proof of the theorem.

Let  $I = \{1, 2, \dots, L\}$  and  $J = \{L+1, L+2, \dots, C\}$ . Because  $\mathbf{z}$  is sorted,  $\forall i \in I, j \in J$  we have  $z_i > z_j$ . Therefore, according to the auxiliary lemma:  $\exp(z_i) \cdot \exp(z_j/T) \geq \exp(z_i/T) \cdot \exp(z_j)$ . Consequently, the following holds:

$$\begin{aligned} \sum_{i=1}^L \sum_{j=L+1}^C \exp(z_i) \cdot \exp(z_j/T) &\geq \sum_{i=1}^L \sum_{j=L+1}^C \exp(z_i/T) \cdot \exp(z_j) \\ &\Downarrow \\ \sum_{i=1}^L \exp(z_i) \cdot \sum_{j=L+1}^C \exp(z_j/T) &\geq \sum_{i=1}^L \exp(z_i/T) \cdot \sum_{j=L+1}^C \exp(z_j). \end{aligned}$$

Adding  $\sum_{i=1}^L \exp(z_i) \cdot \sum_{j=1}^L \exp(z_j/T)$  to both sides, we get

$$\sum_{i=1}^L \exp(z_i) \sum_{j=L+1}^C \exp(z_j/T) + \sum_{i=1}^L \exp(z_i) \sum_{j=1}^L \exp(z_j/T) \geq \sum_{i=1}^L \exp(z_i/T) \sum_{j=L+1}^C \exp(z_j) + \sum_{i=1}^L \exp(z_i) \sum_{j=1}^L \exp(z_j/T),$$

which can be written as

$$\begin{aligned} \sum_{i=1}^L \exp(z_i) \left[ \sum_{i=1}^L \exp(z_i/T) + \sum_{j=L+1}^C \exp(z_j/T) \right] &\geq \sum_{j=1}^L \exp(z_j/T) \left[ \sum_{i=1}^L \exp(z_i) + \sum_{j=L+1}^C \exp(z_j) \right] \\ &\Downarrow \\ \sum_{i=1}^L \exp(z_i) \sum_{j=1}^C \exp(z_j/T) &\geq \sum_{i=1}^L \exp(z_i/T) \sum_{j=1}^C \exp(z_j) \\ &\Downarrow \\ \frac{\sum_{i=1}^L \exp(z_i)}{\sum_{j=1}^C \exp(z_j)} &\geq \frac{\sum_{i=1}^L \exp(z_i/T)}{\sum_{j=1}^C \exp(z_j/T)} \\ &\Downarrow \\ \sum_{j=1}^L \frac{\exp(z_j)}{\sum_{c=1}^C \exp(z_c)} &\geq \sum_{j=1}^L \frac{\exp(z_j/T)}{\sum_{c=1}^C \exp(z_c/T)} \end{aligned}$$

as stated in the theorem. Note that the inequality is strict unless  $L = C$  (both sides equal 1) or  $T = 1$  or  $z_1 = \dots = z_C$  (all the pairs are equal).  $\square$

**Corollary A.3.** *The threshold value  $\hat{q}$  of the non-randomized version of APS and RAPS decreases monotonically as the temperature  $T$  increases above 1.*

*Proof.* Let us start with APS. Set  $T \geq 1$ . For each sample  $(\mathbf{x}, y)$  in the CP set, we get the post softmax vectors  $\hat{\pi}_T$  and  $\hat{\pi}$ , with and without TS, respectively. By Theorem A.2, applied on the sorted vector  $\boldsymbol{\pi} = [\hat{\pi}_{(1)}, \dots, \hat{\pi}_{(C)}]^\top$  with  $L = L_y$  (the index that  $y$  is permuted to after sorting), we have that

$$\sum_{i=1}^{L_y} \hat{\pi}_{(i)}(\mathbf{x}) \geq \sum_{i=1}^{L_y} \hat{\pi}_{T,(i)}(\mathbf{x}). \quad (7)$$

That is, the score of APS decreases *universally* for each sample in the CP set. This implies that  $\hat{q}$ , the  $\frac{[(n+1)(1-\alpha)]}{n}$  quantile of the scores of the samples of the CP set, decreases as well.

The statement can be extended to monotonic decrease simply but observing that for each  $T_2 \geq T_1 \geq 1$  we can apply Theorem A.2 with  $\boldsymbol{\pi} = [\hat{\pi}_{T_1,(1)}, \dots, \hat{\pi}_{T_1,(C)}]^\top$  and  $T = T_2/T_1 \geq 1$ .

We turn to consider RAPS. In this case, a decrease due to TS in the score of each sample  $(\mathbf{x}, y)$  in the CP set, i.e.,

$$\sum_{i=1}^{L_y} \hat{\pi}_{(i)}(\mathbf{x}) + \lambda(L_y - k_{reg})_+ \geq \sum_{i=1}^{L_y} \hat{\pi}_{T,(i)}(\mathbf{x}) + \lambda(L_y - k_{reg})_+,$$

simply follows from adding  $\lambda(L_y - k_{reg})_+$  to both sides of (7). The rest of the arguments are exactly as in APS.  $\square$

**Theorem A.4.** *Let  $\boldsymbol{\pi} \in \Delta^{C-1}$  be a probability vector with  $\pi_i > 0$ , and mean  $\bar{\pi} = \frac{1}{C} \sum_{i=1}^C \pi_i$ . Consider the function  $g(\boldsymbol{\pi}; T, L) = \sum_{i=1}^L \pi_i - \sum_{i=1}^L \sigma_i(\frac{1}{T} \ln \boldsymbol{\pi})$ , where  $\boldsymbol{\sigma}(\cdot)$  is the softmax function. Let  $L \in [C-1]$  and  $\mathbf{r} = [\delta, -\frac{1}{C-1}\delta, \dots, -\frac{1}{C-1}\delta]^\top$  with some  $\delta > 0$ . If*

$$T > \frac{C\sqrt{L}}{(C-L)\pi_1} + \frac{\sqrt{L}}{(C-L)} \left\| [\pi_1^{-1} - \bar{\pi}^{-1}, \dots, \pi_C^{-1} - \bar{\pi}^{-1}] \right\|_2$$

then

$$\mathbf{r}^\top \nabla_{\boldsymbol{\pi}} g(\boldsymbol{\pi}; T, L) > 0.$$

*Proof.* Denote  $\boldsymbol{\pi}^{-1} = [1/\pi_1, \dots, 1/\pi_C]^\top$ . Denote also  $\boldsymbol{\pi}_T = \boldsymbol{\sigma}(\frac{1}{T} \ln \boldsymbol{\pi})$  and  $\mathbf{J}_{\boldsymbol{\pi}_T} = \text{diag}(\boldsymbol{\pi}_T) - \boldsymbol{\pi}_T \boldsymbol{\pi}_T^\top$  (which is the Jacobian of the softmax at the point  $\frac{1}{T} \ln \boldsymbol{\pi}$ ). Denote by  $\mathbf{1}_{1:L}$  the vector in  $\mathbb{R}^C$  with ones in its first  $L$  entries and zeros elsewhere.

Using the chain rule, we have that

$$\nabla g(\boldsymbol{\pi}; T, L) = \mathbf{1}_{1:L} - \frac{1}{T} \text{diag}(\boldsymbol{\pi}^{-1}) (\text{diag}(\boldsymbol{\pi}_T) - \boldsymbol{\pi}_T \boldsymbol{\pi}_T^\top) \mathbf{1}_{1:L} = \mathbf{1}_{1:L} - \frac{1}{T} \text{diag}(\boldsymbol{\pi}^{-1}) \mathbf{J}_{\boldsymbol{\pi}_T} \mathbf{1}_{1:L}.$$

Therefore,

$$\begin{aligned}
 \mathbf{r}^\top \nabla g(\boldsymbol{\pi}; T, L) &= (1 - \frac{L-1}{C-1})\delta - \frac{\delta}{T} \left[ \frac{1}{\pi_1}, -\frac{1}{(C-1)\pi_2}, \dots, -\frac{1}{(C-1)\pi_C} \right] \mathbf{J}_{\boldsymbol{\pi}_T} \mathbf{1}_{1:L} \\
 &= \frac{C-L}{C-1}\delta - \frac{\delta}{T} \left( \left[ \frac{C}{(C-1)\pi_1}, 0, \dots, 0 \right] - \frac{1}{(C-1)} (\boldsymbol{\pi}^{-1})^\top \right) \mathbf{J}_{\boldsymbol{\pi}_T} \mathbf{1}_{1:L} \\
 &= \frac{C-L}{C-1}\delta - \frac{\delta}{T(C-1)} \left( \left[ \frac{C}{\pi_1}, 0, \dots, 0 \right] - \left( \boldsymbol{\pi}^{-1} - \frac{1}{\bar{\pi}} \mathbf{1}_C \right)^\top \right) \mathbf{J}_{\boldsymbol{\pi}_T} \mathbf{1}_{1:L} \\
 &\geq \frac{C-L}{C-1}\delta - \frac{\delta C}{T(C-1)\pi_1} \|\mathbf{J}_{\boldsymbol{\pi}_T}\|_{op} \|\mathbf{1}_{1:L}\|_2 - \frac{\delta}{T(C-1)} \|\mathbf{J}_{\boldsymbol{\pi}_T}\|_{op} \left\| \boldsymbol{\pi}^{-1} - \frac{1}{\bar{\pi}} \mathbf{1}_C \right\|_2 \|\mathbf{1}_{1:L}\|_2 \\
 &\geq \frac{C-L}{C-1}\delta - \frac{\delta C \sqrt{L}}{T(C-1)\pi_1} - \frac{\delta \sqrt{L}}{T(C-1)} \left\| \left[ \frac{1}{\pi_1} - \frac{1}{\bar{\pi}}, \dots, \frac{1}{\pi_C} - \frac{1}{\bar{\pi}} \right] \right\|_2 \\
 &> 0
 \end{aligned}$$

where the third equality uses that fact that adding the subtracted vector would simply vanish:  $\frac{1}{\bar{\pi}} \mathbf{1}_C^\top \mathbf{J}_{\boldsymbol{\pi}_T} = \mathbf{0}^\top$ , the second inequality uses  $\|\mathbf{J}_{\boldsymbol{\pi}_T}\|_{op} \leq 1$ , as shown below, and the last inequality uses the advertised bound on  $T$ .

It is left to show that  $\|\mathbf{J}_{\boldsymbol{\pi}_T}\|_{op} \leq 1$ . This follows from the fact that for any  $\mathbf{u} \in \mathbb{R}^C$  we have

$$\mathbf{u}^\top \mathbf{J}_{\boldsymbol{\pi}_T} \mathbf{u} = \sum_{i=1}^C \pi_{T,i} u_i^2 - \left( \sum_{i=1}^C \pi_{T,i} u_i \right)^2 \leq \sum_{i=1}^C \pi_{T,i} u_i^2 \leq \sup_i (\pi_{T,i}) \sum_{i=1}^C u_i^2 \leq \|\mathbf{u}\|_2^2.$$

Namely, the largest eigenvalue of  $\mathbf{J}_{\boldsymbol{\pi}_T}$  cannot be larger than 1. □

**Proposition A.5.** Consider  $\hat{\boldsymbol{\pi}}, \hat{\boldsymbol{\pi}}_T \in \Delta^{C-1}$ , and  $\hat{q}, \hat{q}_T \in [0, 1]$  such that  $\hat{q} \geq \hat{q}_T$ . Let  $L = \min\{l : \sum_{i=1}^l \hat{\pi}_i \geq \hat{q}\}$ ,

$L_T = \min\{l : \sum_{i=1}^l \hat{\pi}_{T,i} \geq \hat{q}_T\}$ . The following holds:

$$\forall M \in [L] : \sum_{i=1}^M \hat{\pi}_i - \sum_{i=1}^M \hat{\pi}_{T,i} \geq \hat{q} - \hat{q}_T \implies L \leq L_T.$$

*Proof.*  $\forall M \in [L] : \sum_{i=1}^M \hat{\pi}_i - \sum_{i=1}^M \hat{\pi}_{T,i} \geq \hat{q} - \hat{q}_T \iff \forall M \in [L] : \sum_{i=1}^M \hat{\pi}_i \geq \hat{q} - \hat{q}_T + \sum_{i=1}^M \hat{\pi}_{T,i}$

Note that for every  $x \leq \hat{q}$  we have  $M_x := \min\{l : \sum_{i=1}^l \hat{\pi}_i \geq x\} \leq L$ . For  $M_x > 1$  (i.e., not minimal possible value), the

event implies  $\hat{q} - \hat{q}_T + \sum_{i=1}^{M_x-1} \hat{\pi}_{T,i} \leq \sum_{i=1}^{M_x-1} \hat{\pi}_i < x$ . This implies that  $\min\{l : \hat{q} - \hat{q}_T + \sum_{i=1}^l \hat{\pi}_{T,i} \geq x\}$  cannot be smaller than  $M_x$ . That is,

$$\implies \forall x \leq \hat{q} : \min\{l : \sum_{i=1}^l \hat{\pi}_i \geq x\} \leq \min\{l : \hat{q} - \hat{q}_T + \sum_{i=1}^l \hat{\pi}_{T,i} \geq x\}$$

Let us pick  $x = \hat{q}$ :

$$\min\{l : \sum_{i=1}^l \hat{\pi}_i \geq \hat{q}\} \leq \min\{l : \hat{q} - \hat{q}_T + \sum_{i=1}^l \hat{\pi}_{T,i} \geq \hat{q}\}$$

$$\iff \min\{l : \sum_{i=1}^l \hat{\pi}_i \geq \hat{q}\} \leq \min\{l : \sum_{i=1}^l \hat{\pi}_{T,i} \geq \hat{q}_T\} \iff L \leq L_T$$

□

**Proposition A.6.** Let  $\mathbf{z} \in \mathbb{R}^C$  and  $\sigma(\cdot)$  be the softmax function. Consider Shannon's entropy  $H : \Delta^{C-1} \rightarrow \mathbb{R}$ , i.e.,  $H(\boldsymbol{\pi}) = -\sum_{i=1}^C \pi_i \ln(\pi_i)$ . Unless  $\mathbf{z} \propto \mathbf{1}_C$  (then  $\sigma(\mathbf{z}/T) = \sigma(\mathbf{z})$ ), we have that  $H(\sigma(\mathbf{z}/T))$  is strictly monotonically increasing as  $T$  grows.

*Proof.* To prove this statement, let us show that the function  $f(T) = H(\sigma(\mathbf{z}/T))$  monotonically increases (as  $T$  increases, regardless of  $\mathbf{z}$ ). To achieve this, we need to show that  $f'(T) = \frac{d}{dT} H(\sigma(\mathbf{z}/T)) \geq 0$ .

By the chain-rule,  $f'(T) = \frac{d}{dT} (H(\sigma(\mathbf{z}/T))) = \frac{\partial H(\boldsymbol{\sigma})}{\partial \boldsymbol{\sigma}} \frac{\partial \boldsymbol{\sigma}(\mathbf{z})}{\partial \mathbf{z}} \frac{\partial}{\partial T} (\mathbf{z}/T)$ . Let us compute each term:

$$\begin{aligned} \frac{\partial H(\boldsymbol{\sigma})}{\partial \sigma_i} &= -\ln(\sigma_i) - \frac{1}{\sigma_i} \cdot \sigma_i = -\ln(\sigma_i) - 1 \implies \frac{\partial H(\boldsymbol{\sigma})}{\partial \boldsymbol{\sigma}} = -\ln(\boldsymbol{\sigma})^\top - \mathbf{1}_C^\top \\ \frac{\partial \sigma_i(\mathbf{z})}{\partial z_j} &= \sigma_i(\mathbf{z}) \cdot (\mathbb{I}\{i=j\} - \sigma_j(\mathbf{z})) \implies \frac{\partial \boldsymbol{\sigma}(\mathbf{z})}{\partial \mathbf{z}} = \text{diag}(\boldsymbol{\sigma}(\mathbf{z})) - \boldsymbol{\sigma}(\mathbf{z})\boldsymbol{\sigma}(\mathbf{z})^\top \\ \frac{\partial}{\partial T} (\mathbf{z}/T) &= -\frac{1}{T^2} \mathbf{z} \end{aligned}$$

where in  $\ln(\boldsymbol{\sigma})$  the function operates entry-wise and  $\mathbb{I}\{i=j\}$  is the indicator function (equals 1 if  $i=j$  and 0 otherwise).

Next, observe that  $\mathbf{1}_C^\top (\text{diag}(\boldsymbol{\sigma}) - \boldsymbol{\sigma}\boldsymbol{\sigma}^\top) = \boldsymbol{\sigma}^\top - \boldsymbol{\sigma}^\top = \mathbf{0}^\top$ . Consequently, we get

$$\begin{aligned} \frac{d}{dT} (H(\sigma(\mathbf{z}/T))) &= \frac{1}{T^2} \ln(\boldsymbol{\sigma}(\mathbf{z}))^\top (\text{diag}(\boldsymbol{\sigma}(\mathbf{z})) - \boldsymbol{\sigma}(\mathbf{z})\boldsymbol{\sigma}(\mathbf{z})^\top) \mathbf{z} \\ &= \frac{1}{T^2} (\mathbf{z} - s(\mathbf{z})\mathbf{1}_C)^\top (\text{diag}(\boldsymbol{\sigma}(\mathbf{z})) - \boldsymbol{\sigma}(\mathbf{z})\boldsymbol{\sigma}(\mathbf{z})^\top) \mathbf{z} \\ &= \frac{1}{T^2} \mathbf{z}^\top (\text{diag}(\boldsymbol{\sigma}(\mathbf{z})) - \boldsymbol{\sigma}(\mathbf{z})\boldsymbol{\sigma}(\mathbf{z})^\top) \mathbf{z} \end{aligned}$$

where in the second equality we used  $[\ln(\boldsymbol{\sigma}(\mathbf{z}))]_i = \ln\left(\frac{\exp(z_i)}{\sum_{j=1}^C \exp(z_j)}\right) = z_i - s(\mathbf{z})$ , where  $s(\mathbf{z}) = \ln\left(\sum_{j=1}^C \exp(z_j)\right)$ .

Therefore, for establishing that  $\frac{d}{dT} (H(\sigma(\mathbf{z}/T))) \geq 0$ , we can show that  $(\text{diag}(\boldsymbol{\sigma}) - \boldsymbol{\sigma}\boldsymbol{\sigma}^\top)$  is a positive semi-definite matrix. Let  $\tilde{\sigma}_i = \exp(z_i)$  and notice that  $\sigma_i = \frac{\tilde{\sigma}_i}{\sum_{j=1}^C \tilde{\sigma}_j}$ . Indeed, for any  $\mathbf{u} \in \mathbb{R}^C \setminus \{\mathbf{0}\}$  we have that

$$\begin{aligned} \mathbf{u}^\top (\text{diag}(\boldsymbol{\sigma}) - \boldsymbol{\sigma}\boldsymbol{\sigma}^\top) \mathbf{u} &= \sum_{i=1}^C u_i^2 \sigma_i - \left(\sum_{i=1}^C u_i \sigma_i\right)^2 \\ &= \frac{\sum_{i=1}^C u_i^2 \tilde{\sigma}_i \cdot \sum_{j=1}^C \tilde{\sigma}_j - \left(\sum_{i=1}^C u_i \tilde{\sigma}_i\right)^2}{\left(\sum_{j=1}^C \tilde{\sigma}_j\right)^2} \\ &\geq 0, \end{aligned}$$

where the inequality follows from Cauchy–Schwarz inequality:  $\sum_{i=1}^C u_i \tilde{\sigma}_i = \sum_{i=1}^C u_i \sqrt{\tilde{\sigma}_i} \sqrt{\tilde{\sigma}_i} \leq \sqrt{\sum_{i=1}^C u_i^2 \tilde{\sigma}_i} \sqrt{\sum_{j=1}^C \tilde{\sigma}_j}$ .

Cauchy–Schwarz inequality is attained with equality iff  $u_i \sqrt{\tilde{\sigma}_i} = c \sqrt{\tilde{\sigma}_i}$  with the same constant  $c$  for  $i = 1, \dots, C$ , i.e., when  $\mathbf{u} = c\mathbf{1}_C$ . Recalling that  $\frac{d}{dT} (H(\sigma(\mathbf{z}/T))) = \frac{1}{T^2} \mathbf{z}^\top (\text{diag}(\boldsymbol{\sigma}) - \boldsymbol{\sigma}\boldsymbol{\sigma}^\top) \mathbf{z}$ , this implies that  $\frac{d}{dT} (H(\sigma(\mathbf{z}/T))) = 0 \iff z_1 = \dots = z_C$ , and otherwise  $\frac{d}{dT} (H(\sigma(\mathbf{z}/T))) > 0$ .

□

## B. Additional Empirical Results

In this section, we provide additional figures that present the empirical results for each of the dataset-model pairs in our experiments. For comprehensive details of each experiment, refer to Section 3.

### B.1. Mean prediction set size as function of Temperature $T$ for each of the CP algorithms

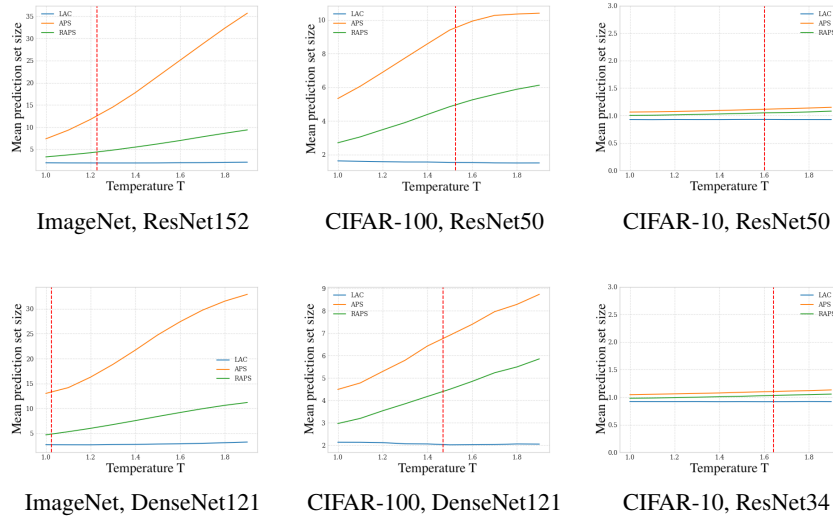


Figure 6. Mean prediction set size for LAC, APS and RAPS versus the temperature  $T$ .

### B.2. Mean threshold value $\hat{q}$ generated by each of the algorithms as function of the temperature $T$

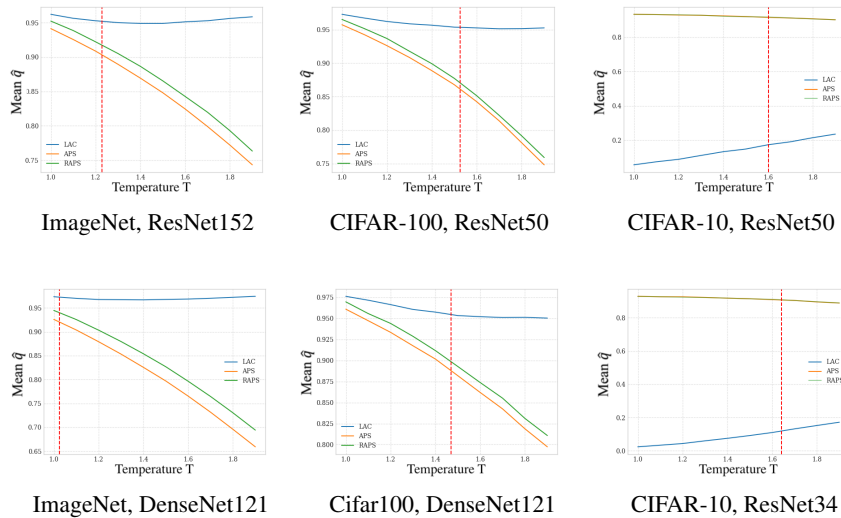


Figure 7. Mean threshold  $\hat{q}$  for LAC, APS and RAPS versus the temperature  $T$ .



B.3. Reliability diagram before and after TS

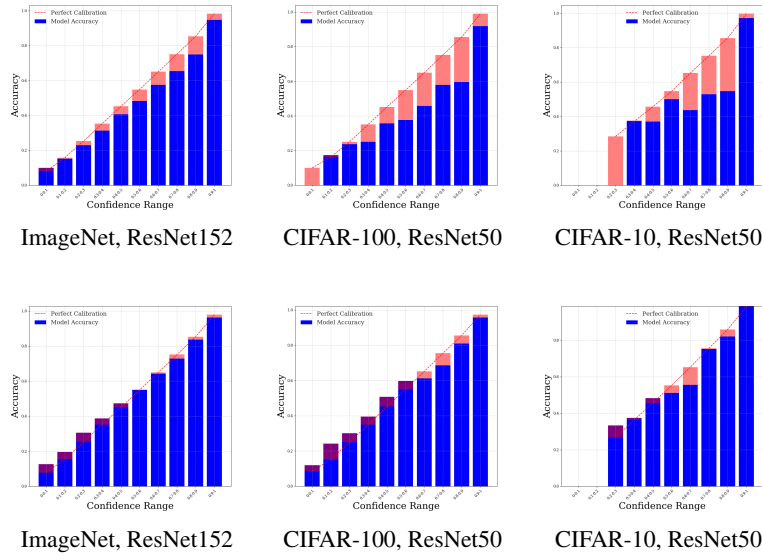


Figure 8. Reliability diagrams before (top) and after (bottom) TS calibration with ECE objective.

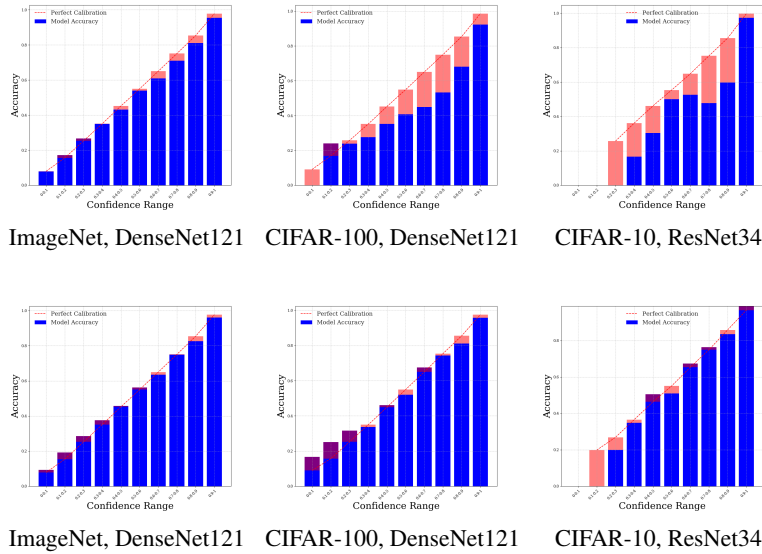
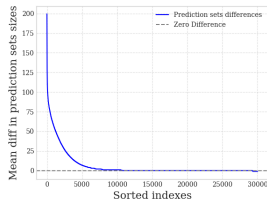
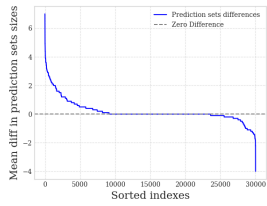


Figure 9. Reliability diagrams before (top) and after (bottom) TS calibration with ECE objective.

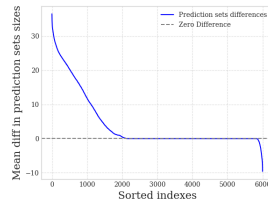
**B.4. Sorted prediction sets sizes differences (with TS minus without TS)**



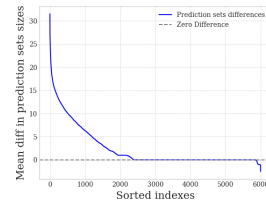
ImageNet, ResNet152 - APS algorithm



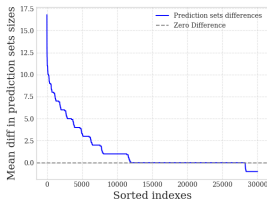
ImageNet, DenseNet121 - APS algorithm



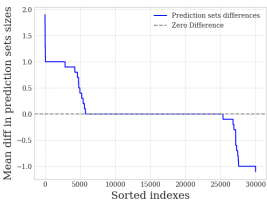
CIFAR-100, ResNet50 - APS algorithm



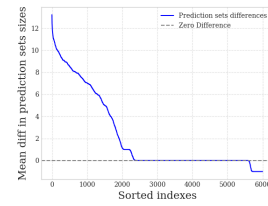
CIFAR-100, DenseNet121 - APS algorithm



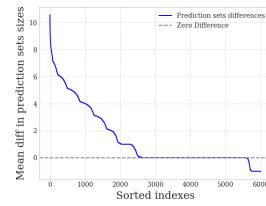
ImageNet, ResNet152 - RAPS algorithm



ImageNet, DenseNet121 - RAPS algorithm



CIFAR-100, ResNet50 - RAPS algorithm



CIFAR-100, DenseNet121 - RAPS algorithm

**B.5. Optimal temperature  $T$  for NLL and ECE criteria**

Table 4. Optimal Temperature for NLL and ECE criteria

| Dataset-Model          | Optimal T<br>- NLL loss | Optimal T<br>- ECE loss |
|------------------------|-------------------------|-------------------------|
| CIFAR-100, ResNet50    | 1.338                   | 1.524                   |
| CIFAR-100, DenseNet121 | 1.380                   | 1.469                   |
| ImageNet, ResNet152    | 1.207                   | 1.227                   |
| ImageNet, DenseNet121  | 1.054                   | 1.024                   |
| CIFAR-10, ResNet50     | 1.683                   | 1.761                   |
| CIFAR-10, ResNet34     | 1.715                   | 1.802                   |